Nuclear Instruments and Methods in Physics Research B 269 (2011) 804–809

Contents lists available at ScienceDirect

Nuclear Instruments and Methods in Physics Research B

journal homepage: www.elsevier.com/locate/nimb

# Charge-exchange straggling in equilibrium

P. Sigmund [a,*], O. Osmani [b,c], A. Schinner [d]

[a] Department of Physics and Chemistry, University of Southern Denmark, DK-5230 Odense M, Denmark
[b] Department of Physics, University of Duisburg-Essen, D-47048 Duisburg, Germany
[c] Department of Physics, University of Kaiserslautern and Research Center OPTIMAS, D-67653 Kaiserslautern, Germany
[d] Institut für Experimentalphysik, Johannes, Kepler Universität, A-4040 Linz, Austria

ARTICLE INFO

*Article history:*
Received 1 September 2010
Received in revised form 2 November 2010
Available online 13 December 2010

*Keywords:*
Stopping power
Straggling
Charge exchange
Charge equilibrium
Swift heavy ions

ABSTRACT

A general expression has been derived that allows computation of charge-exchange straggling of swift heavy ions when many charge states are involved. Charge exchange is found to hinge on the variation of the stopping cross section with the ion charge and on the transient behavior of the charge population as a function of traveled pathlength. These effects appear factorized in the final formula. The focus of this paper is on straggling in charge equilibrium. The case of MeV/u sulfur ions in carbon has been used as an illustration. Charge-exchange straggling is found to be dominating straggling over a considerable range of beam energies.



## 1. Introduction

Straggling denotes the broadening of the energy-loss spectrum of a beam of charged particles with increasing penetration depth [1]. Theoretical understanding of straggling has been proceeding slowly over many years because of a considerable number of effects that need to be analyzed. All those processes which determine the mean energy loss, such as excitation and ionization of target electrons, projectile excitation, charge exchange, elastic nuclear collisions, pair creation and bremsstrahlung, contribute potentially to straggling albeit with different weight. In addition there are spatial correlation effects which are specific to straggling.

Charge exchange is known to play a dual role in stopping: firstly, electron capture and loss contribute to the energy balance in individual collisions. Secondly, charge exchange affects the statistics of particle penetration even if the associated energy loss is negligible, since all stopping processes mentioned above depend on the charge state of the penetrating ion. If the charge state fluctuates, energy loss must fluctuate. This affects the mean energy loss and, even more, the straggling.

Charge-exchange straggling has been mentioned early [2] and discussed in the experimental literature [3–5]. Direct evidence emerges from state-specific energy-loss measurements [6–9] and subsequent work by these teams.

The first theoretical studies [3,10] focused on systems with only two charge states. General transport equations for an arbitrary number of states were derived by Winterbon [11], who explicitly studied the case of 15 MeV $I^-$ ions in $O_2$ on the basis of a simple stopping model. Emphasis was laid there on the transient behavior as a function of pathlength. This work made it clear that straggling by charge exchange may well exceed the Bohr prediction [12] of 'collisional straggling'. Experimental evidence showing huge straggling values for swift heavy ions has emerged subsequently [13].

A general expression governing energy-loss spectra in thin layers in the presence of charge exchange was presented in Ref. [14]. This scheme determines the energy-loss spectrum as a function of entrance and exit charge from zero thickness up to charge equilibrium. General expressions were derived for mean energy loss and variance, including transient behavior [14,15]. The expression found in Ref. [3] for a 2-state system was generalized, and an explicit expression was derived also for a 3-state system [14]. The scheme was applied primarily to state-specific energy-loss spectra for quasi-two-state systems as a function of thickness in Ref. [16] and subsequent studies.

The treatment offered in Refs. [14,15] makes heavy use of an eigenvalue expansion. This was found to be useful in a general analysis but less convenient in practical calculations. The present treatment, based on Ref. [14], is geared toward systems with many charge states where a continuum description appears justified.

## 2. Recapitulation

### 2.1. General

The energy-loss spectrum of a penetrating ion as a function of pathlength $x$ is expressed as a matrix [14]

* Corresponding author.

0168-583X/$ - see front matter © 2010 Elsevier B.V. All rights reserved.
doi:10.1016/j.nimb.2010.11.094

$$\mathbf{F}(\Delta E, x) = ||F_{IJ}(\Delta E, x)||, \tag{1}$$

where $I$ and $J$ denote the state of the ion at depth 0 and $x$, respectively. Talking about 'states' instead of 'charge states' allows to include excitation states of the ion. $\mathbf{F}(\Delta E, x)$ can be expressed as a Bothe–Landau integral [14],

$$\mathbf{F}(\Delta E, x) = \frac{1}{2\pi}\int_{-\infty}^{\infty} dk e^{ik\Delta E} e^{Nx\mathbf{Q}(k)}, \tag{2}$$

where $N$ is the number of atoms per volume and $\mathbf{Q}(k)$ a matrix with the elements

$$Q_{IJ}(k) = Q_{IJ} - \int d\sigma_{IJ}(T)\left(1 - e^{-ikT}\right); \tag{3}$$

$$Q_{IJ} = \sigma_{IJ} - \delta_{IJ}\sum_L \sigma_{IL}. \tag{4}$$

Here $d\sigma_{IJ}(T)$ is the differential cross section for energy loss $(T, dT)$ and transition from $I$ to $J$ and $\sigma_{IJ} = \int d\sigma_{IJ}(T)$ the total transition cross section.

Eq. (4) assumes that consecutive collisions are separated in space and take place at random intervals, and that the total energy loss during passage through pathlength $x$ is small so that cross sections can be assumed independent of pathlength. One may question the validity of the first assumption in case of a dense medium. An attempt to take into account quantum interferences in charge-state statistics has been made in Ref. [17]. The second restriction is more technical and can, if necessary, be circumvented by division into sublayers and subsequent convolution.

### 2.2. Moments

The zeroth moment over $\mathbf{F}(\Delta E, x)$ delivers the charge fractions $F_{IJ}(x)$. The first moment delivers the mean energy loss summed over all exit states,

$$\left(\frac{d\langle\Delta E\rangle}{Ndx}\right)_I = \sum_J F_{IJ}(x) S_J, \tag{5}$$

where $S_J = \sum_L S_{JL}$ is the total stopping cross section of an ion in state $J$ and

$$S_{JL} = \int T\, d\sigma_{JL}(T) \tag{6}$$

a partial stopping cross section. The expression

$$\left(\frac{d\langle\Delta E^2\rangle}{Ndx}\right)_I = \sum_J F_{IJ}(x) W_J + 2\sum_{JKL} N\int_0^x dx'\, F_{IJ}(x-x') S_{JK} F_{KL}(x') S_L \tag{7}$$

can be extracted for the second moment from Ref. [14], where $W_J = \sum_L W_{JL}$, and

$$W_{JL} = \int T^2\, d\sigma_{JL}(T) \tag{8}$$

is a partial straggling parameter.

## 3. Straggling

The variance over the energy-loss profile follows from Eqs. (7) and (5),

$$\frac{d}{Ndx}\left(\left\langle\Delta E^2\right\rangle_I - \langle\Delta E\rangle_I^2\right) = \sum_J F_{IJ}(x) W_J + \frac{d\Delta\Omega_I^2}{Ndx}, \tag{9}$$

where

$$\frac{d\Delta\Omega_I^2}{Ndx} = 2\sum_{JKL} N\int_0^x dx'\, F_{IJ}(x-x') S_{JK}[F_{KL}(x') - F_{IL}(x)] S_L \tag{10}$$

represents charge-exchange straggling. This expression is exact within the assumptions specified above.

With increasing pathlength $x$ the memory is lost, so that

$$F_{IJ}(x) \to F_J \text{ for } x \gg \Lambda, \tag{11}$$

where $F_J$ is the equilibrium fraction in state $J$ and $\Lambda$ an equilibration distance. For $x \gg \Lambda$ the integrand in Eq. (10) is nonvanishing for $x' \lesssim \Lambda$ and can therefore be replaced by $F_J[F_{KL}(x') - F_L]$, so that

$$\frac{d\Delta\Omega^2}{Ndx} = 2N\sum_{JKL} F_J S_{JK} S_L \int_0^\infty dx\, (F_{KL}(x) - F_L) \tag{12}$$

for $x \gg \Lambda$, independent of the initial state $I$.

## 4. Continuum approximation

### 4.1. Stopping cross section

The approximation will be made that the stopping cross section $S_J$ only depends on the instantaneous ion charge $q_J$, i.e.,

$$S_J = S(q_J). \tag{13}$$

This implies that the effect of the detailed arrangement of the projectile electrons *on the energy loss* is neglected. An indication of the accuracy of this approximation may be found in Ref. [18], Fig. 6, where the difference between stopping cross sections for Ni in C, evaluated for two projectile configurations reflecting the same charge state, is barely visible. The influence of the electron configuration on *charge-exchange cross sections* is unquestionably greater than on energy-loss cross sections.

In charge equilibrium the charge state fluctuates around its mean value

$$q = \sum_J q_J F_J. \tag{14}$$

In the following it will be assumed that the dependence of the stopping cross section on the instantaneous ion charge can be approximated as

$$S_J \simeq s_0 + (q_J - q)s_1 + \frac{1}{2}(q_J - q)^2 s_2 \tag{15}$$

where

$$s_0 = S(q); \quad s_1 = \left.\frac{dS}{dq_J}\right|_{q_J=q}; \quad s_2 = \left.\frac{d^2S}{dq_J^2}\right|_{q_J=q}. \tag{16}$$

The quantities $s_0$, $s_1$ and $s_2$ depend only on $q$, i.e., on the beam energy for a given ion-target combination.

Fig. 1 illustrates Eq. (15) on a representative example. The stopping cross section for 1 MeV/u $Br^{q+}$ ions in Ne has been calculated for a number of charge states by means of the PASS code, which implements binary stopping theory [18,19]. Similar results have been found by experiments [9] and other computational schemes [20,21]. It is evident that already a linear approximation, which was utilized in Ref. [22] in the analysis of charge fractions, may be well justified. By adding a quadratic term a near-perfect fit is obtained.

Adopting Eq. (15) one finds

$$\sum_L \int_0^\infty dx\, (F_{KL}(x) - F_L) S_L = (s_1 - q s_2)\beta_K + \frac{1}{2}s_2\gamma_K, \tag{17}$$

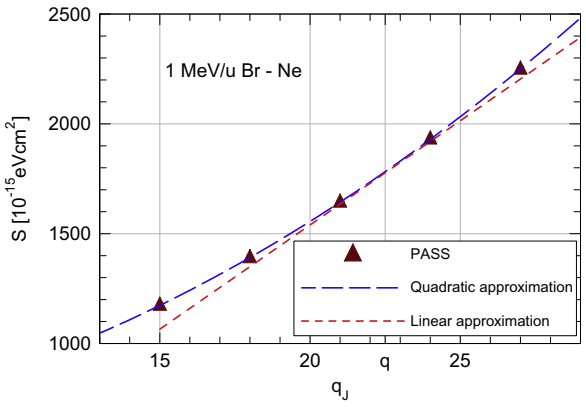


**Fig. 1.** Stopping cross section for 1 MeV/u $Br^{q_J+}$ ions in Ne calculated by the PASS code [18]. Target excitation/ionization only. Also included are a linear and a quadratic approximation, Eq. (15). $q = 22.5$ is the mean equilibrium charge at 1 MeV/u according to ETACHA [24].

where

$$\beta_K = \sum_L q_L \int_0^\infty dx\ (F_{KL}(x) - F_L) \tag{18}$$

and

$$\gamma_K = \sum_L q_L^2 \int_0^\infty dx\ (F_{KL}(x) - F_L). \tag{19}$$

The term proportional to $s_0$ drops out because of the sum rule $\sum_J F_J = 1$. With this, Eq. (12) reduces to

$$\frac{d\Delta\Omega^2}{Ndx} = 2N \sum_{JK} F_J S_{JK} \left[ (s_1 - q s_2)\beta_K + \frac{1}{2} s_2 \gamma_K \right] \tag{20}$$

for $x \gg \Lambda$. In the present explorative study mainly the linear approximation in Eq. (17) has been employed. The correction due to the second-order term is a few per cent in cases investigated explicitly. Then Eq. (20) reduces to

$$\frac{d\Delta\Omega^2}{Ndx} = 2N s_1 \sum_{JK} F_J S_{JK} \beta_K. \tag{21}$$

### 4.2. Diagonal and off-diagonal contributions

It is tempting to apply the approximation (15) also to the partial stopping cross sections $S_{JK}$. Here it is advisable to split Eq. (20) into diagonal, $J = K$, and off-diagonal terms, $J \neq K$. For the diagonal terms Eq. (21) reduces to

$$\left(\frac{d\Delta\Omega^2}{Ndx}\right)_{\text{diag}} = 2N s_1 s_1^{\text{diag}} \sum_J F_J (q_J - q)\beta_J \tag{22}$$

in the linear approximation, where $s_1^{\text{diag}}$ relates to $S_{JJ}$ as $s_1$ relates to $S_J$. The lowest-order term $\propto s_1 s_0^{\text{diag}}$ has dropped out because

$$\sum_J F_J F_{JL}(x) = F_L, \tag{23}$$

which expresses the fact that the equilibrium distribution does not change with increasing pathlength.

Off-diagonal terms represent energy loss by charge exchange. Such terms are often neglected altogether. Keeping them nevertheless for a while, one may simplify the situation by only taking into account one-electron capture and loss events. Dropping all terms with $K \neq J \pm 1$ one finds

$$\left(\frac{d\Delta\Omega^2}{Ndx}\right)_{\text{off}} = 2N s_1 \sum_J \beta_J \left[ F_{J-1} S_{J-1,J} + F_{J+1} S_{J+1,J} \right]. \tag{24}$$

Here the quantity within the parentheses depends on $J$. One may assume a dependence analogous to Eq. (15),

$$F_{J-1} S_{J-1,J} + F_{J+1} S_{J+1,J} \simeq F_J \left[ s_0^{\text{off}}(q) + (q_J - q) s_1^{\text{off}} \ldots \right], \tag{25}$$

even though the continuum description may be less accurate here when $q$ approaches a closing or opening shell.

After addition of this to Eq. (22), Eq. (21) reads

$$\frac{d\Delta\Omega^2}{Ndx} = 2N s_1 s_1' \sum_J F_J (q_J - q)\beta_J, \tag{26}$$

where

$$s_1' = s_1^{\text{diag}} + s_1^{\text{off}}. \tag{27}$$

## 5. Evaluation

Eq. (26) is seen to be composed of a factor $s_1 s_1'$ governed by the stopping dynamics and a factor

$$G_0 = \sum_J F_J (q_J - q)\beta_J \tag{28}$$

governed by the statistics of charge exchange. In the following example, energy loss by charge exchange will be neglected, so that the energy-loss factor reduces to

$$s_1 s_1' \simeq \left[ \left( \frac{dS}{dq_J} \right)_{q_J = q} \right]^2. \tag{29}$$

### 5.1. Influence of the stopping cross section

The quantity $s_1 = dS^{\text{diag}}/dqJ|_{qJ=q}$ has been determined by means of the PASS code [18,19] via $s_1 = S(q_+) - S(q_-)$, where $q_-$ and $q_+$ are the neighboring integer charge states surrounding the equilibrium charge $q$.

Fig. 2 shows $s_1^2$ for He, S, and U ions in carbon over four orders of magnitude in beam energy. Also included is the square of the equilibrium stopping cross section $S$ for the respective ions. The two quantities show qualitatively a similar behavior, but the variation of $s_1^2$ with $Z_1$ is less dramatic than that of $S^2$.

### 5.2. Influence of charge-exchange statistics

This section focuses on the factor $G_0$ defined in Eq. (28). The first step in the development of a comprehensive code, based on charge-state statistics starting from $\mathbf{F}(x) = \exp(Nx\mathbf{Q})$, is in progress [23]. Preliminary results are reported here based on a manual evaluation for swift sulfur ions in carbon.

Charge fractions have been evaluated from the zeroth moment over Eq. (2). The code presented in Ref. [23] is computationally efficient and accurate, but cross-sectional input is incomplete. In particular, only one projectile state has been allowed for every charge state, and spontaneous processes such as Auger decays have not yet been incorporated.

Alternatively, charge fractions may be evaluated from the ETACHA code [24] which is based on rate equations. Input from atomic-collision physics includes cross sections for electron capture and loss as well as transition probabilities for radiational decay and Auger processes. Data are based on Born approximation (electron loss and excitation) and eikonal approximation (capture).

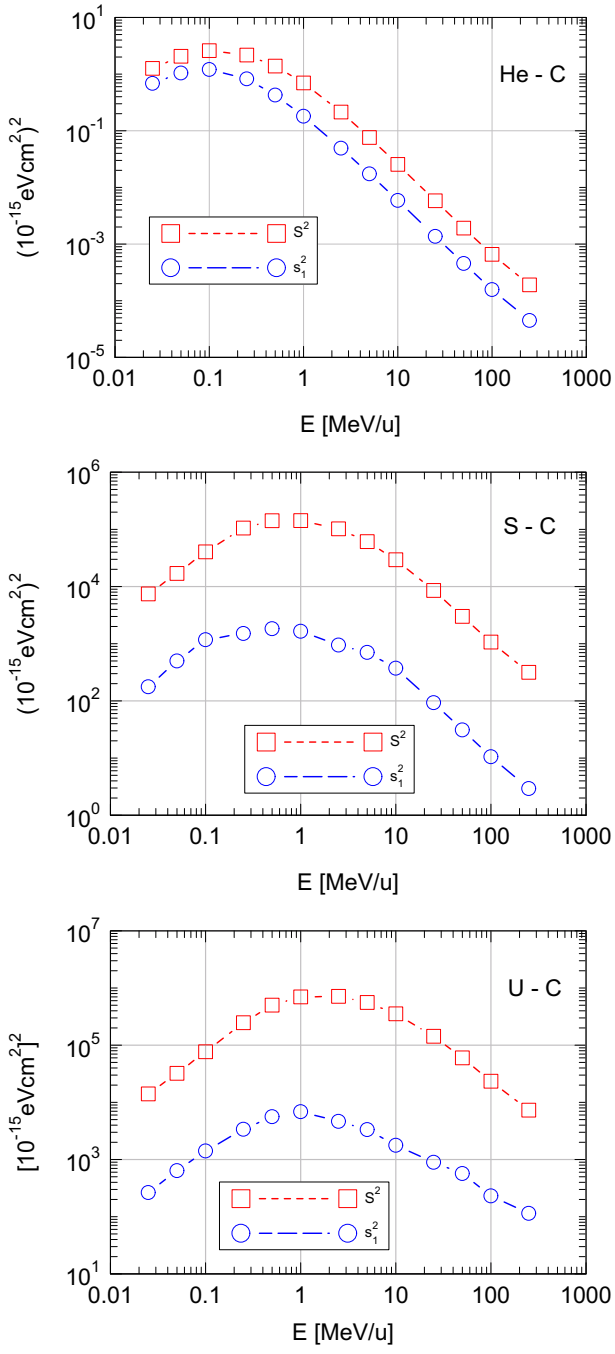


**Fig. 2.** Comparing $S^2$, where $S = s_{0,\text{diag}}$ is the collisional stopping cross section in charge equilibrium, with $s_1^2$, where $s_1 = dS_{\text{diag}}/dq_j|_{q_j=q}$ is the derivative of $S$ with respect to the ion charge. Calculated by the PASS code [18] for He, S and U in C.

The value of $G_0$ has been found to sensitively depend on the quantities $\beta_K$ defined in Eq. (18) as well as the asymptotic charge fractions $F_J$. The accuracy of these quantities is limited firstly by the limited range of validity of the cross-sectional input. The authors of Ref. [24] mention a lower limiting beam energy of 1 MeV/u. Moreover, the ETACHA version available to us is limited to $Z_1 \leqslant 36$. We note that those cross sections that do enter the matrix method are taken from ETACHA.

In contrast to the matrix method, numerical inaccuracies are significant in ETACHA. Charge fractions may show an oscillatory behavior in the equilibrium regime ($x \gg \Lambda$), and even in the absence of such oscillations the value of the asymptotic charge fraction may depend on the initial charge state. Problems associated with these features can be reduced by carefully choosing the upper limit in the integration over $x$ and by verifying that sum rules are obeyed. The case of sulfur ions in carbon has been chosen here, because explicit inspection of all intermediate steps suggests credible results for a rather broad range of beam energies. A systematic evaluation for many ion-target combinations is intended, once the project reported in Ref. [23] has been completed.

Fig. 3 shows the quantity $\beta_K$ defined in Eq. (18) as a function of charge state for a series of beam energies. Fig. 4 shows $\beta_J$ for 1 MeV/u together with the equilibrium charge fraction $F_J$ as well as the product $F_J(q_J - q)\beta_J$ which determines $G_0$ according to Eq. (28).

Fig. 5 shows $G_0$ as a function of the beam energy. It is seen that the results found by ETACHA and the matrix method are similar as far as the shape and the height of the maximum are concerned, whereas they are displaced relative to each other horizontally. The peak positions differ by 2.5 charge units.

This difference appears significant and warrants a decision on what to rely on. In view of the similar shape of the curves we assert that the difference cannot be caused primarily by numerical deficiencies in ETACHA. Conversely, we know from Ref. [23] that the present implementation of the matrix method tends to significantly overestimate the equilibration depth and, hence, may affect the integrals $\beta_J$ over the transients. Moreover, unlike ETACHA, the matrix method overestimates the mean equilibrium charge significantly (Fig. 6) as compared to the common Thomas-Fermi estimate. Therefore we assert that the ETACHA curve is closer to the correct result. We emphasize, however, that the asserted deficien-

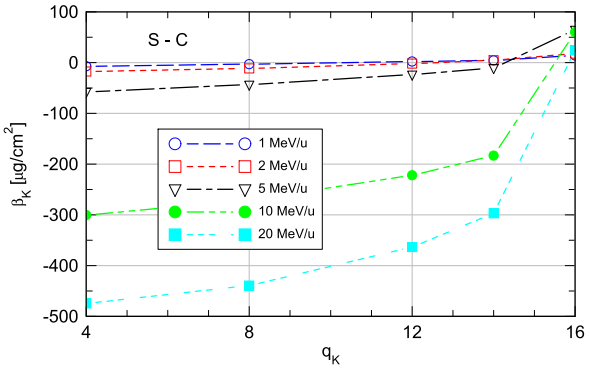


**Fig. 3.** The quantity $\beta_K$ versus ion charge, defined in Eq. (18) and determined by ETACHA for sulfur ions in carbon at five beam energies.

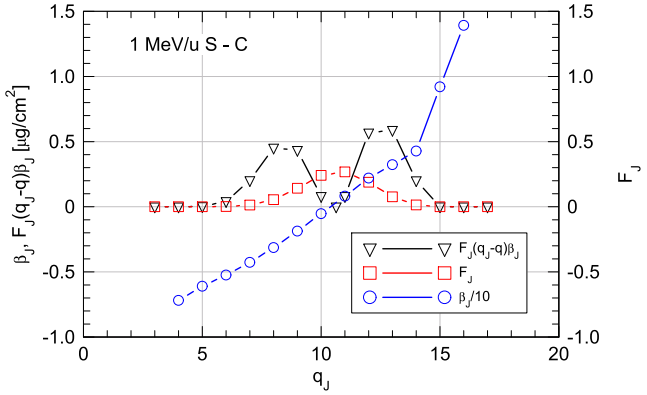


**Fig. 4.** The quantities $\beta_J$, asymptotic charge fraction $F_J$ and the product $F_J(q_J - q)\beta_J$ which determines the factor $G_0$, Eq. (28), for 1 MeV/u S in C as a function of the incoming charge $q_J$. Determined from ETACHA output.

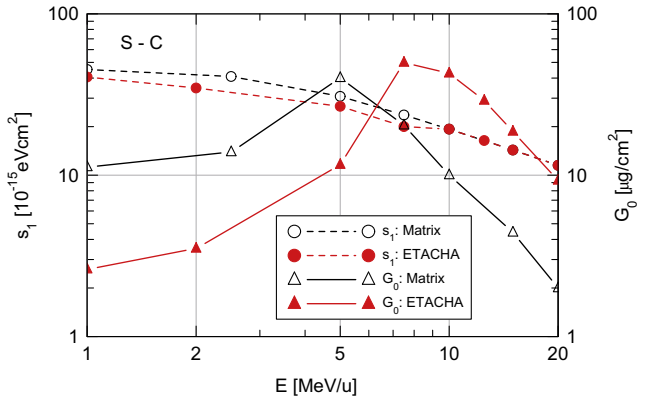


**Fig. 5.** The function $G_0$ determining the straggling correction according to Eq. (28) (solid lines) and the quantity $s_1$ reflecting the variation of the stopping cross section with the charge (broken curves) for S–C. Results found from the matrix method (empty symbols) and from ETACHA (filled symbols).

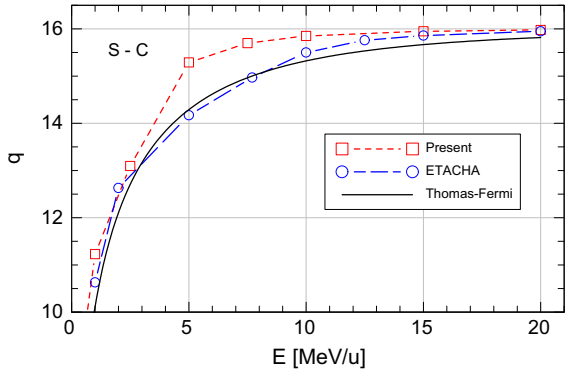


**Fig. 6.** Calculated equilibrium charge for S in C. Squares: matrix method. Circles: ETACHA. Solid line: $q = Z_1[1 - \exp(-v/Z_1^{2/3}v_0)]$.

cies of the matrix method are due to incomplete input rather than to fundamentals of the method.

Fig. 7 shows the correction for charge-exchange straggling resulting from Eq. (26) relative to Bohr straggling,

$$W_{\mathrm{Bohr}} = 4\pi Z_1^2 Z_2 e^4, \tag{30}$$

where $Z_1 = 16$ and $Z_2 = 6$ are atomic numbers of projectile and target, respectively. Most striking is the magnitude of the effect: Adopting the result from ETACHA we find a straggling correction

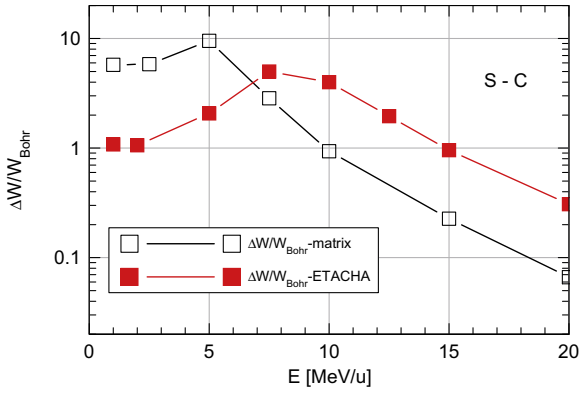


**Fig. 7.** Straggling correction $\Delta W/W_{\mathrm{Bohr}}$ due to charge exchange. Results found from the matrix method (empty symbols) and from ETACHA (solid symbols).

of five times Bohr straggling at 7.5 MeV/u. This is to be compared with a peak value of 0.76 times Bohr straggling due to bunching for Ar in C at 0.5 MeV/u [25]. In accordance with Fig. 5, the general behavior is determined primarily by the charge-state factor $G_0$. Unlike in collisional straggling, in particular bunching and packing [25], the influence of the stopping cross section is of secondary importance.

## 6. Summary

A hierarchy of formulae has been offered, all of which allow computation of charge-exchange straggling. Most general is Eq. (10) which is rigorous within the basic model. Eq. (12) is likewise rigorous but limited to charge equilibrium. Eq. (20), which invokes the continuum description of the total stopping cross section, is asserted to still contain all the essentials, while its linear version Eq. (21) is more approximate. Once the continuum approximation has been made it appears reasonable to go all the way and to apply it to the diagonal and nondiagonal terms of $S_{jk}$. This leads to Eq. (26) or the corresponding second-order relation (not shown).

Eq. (26) is very suited for studying trends, preferably taking into account energy loss by charge exchange in accordance with Eq. (15) or, if the latter is considered negligible, Eq. (21).

An interesting feature which may be hard to extract from the general formulae, Eqs. (10) or (12), but which emerges readily from Eq. (26), is the relative influence of energy-loss dynamics and charge-exchange statistics on charge-exchange straggling. For the system considered in Fig. 5 it appears that the energy dependence is governed primarily by charge-state statistics. If this finding should prove to be more generally valid, it would imply a means of separating straggling by charge exchange from collisional straggling, in particular the bunching effect in collisional straggling.

The numerical part of this study has revealed the importance of accurate input in the form of transient charge fractions $F_{lj}(x)$, whatever the cross-sectional input. Absolute numbers reported here are expected to be subject to modification as the project reported in Ref. [23] develops.

## Acknowledgements

This work has been supported by the Danish Natural Science Research Council (FNU), Deutsche Forschungsgemeinschaft (SFB616) and Research Center OPTIMAS. We are grateful to D. Vernhet and J.P. Rozet for kindly making available their ETACHA code.

## References

[1] P. Sigmund, Particle penetration and radiation effects, vol. 151 of Series in Solid-State Sciences, Springer, Berlin, 2006.
[2] L. Flamm, R. Schumann, Ann. Phys. 50 (1916) 655.
[3] B. Efken, D. Hahn, D. Hilscher, G. Wüstefeld, Nucl. Instrum. Methods 129 (1975) 219.
[4] F. Besenbacher, J.U. Andersen, E. Bonderup, Nucl. Instrum. Methods 168 (1980) 1.
[5] C.J. Sofield, N.E.B. Cowern, J.M. Freeman, Nucl. Instrum. Methods 191 (1981) 462.
[6] J. Cuevas, M. Garcia-Munos, P. Torres, S.K. Allison, Phys. Rev. 135 (1964) A335.
[7] H. Ogawa, I. Katayama, H. Ikegami, Y. Haruyama, A. Aoki, M. Tosaki, F. Fukuzawa, K. Yoshida, I. Sugai, T. Kaneko, Phys. Rev. B 43 (1991) 11370.
[8] C.M. Frey, G. Dollinger, A. Bergmaier, T. Faestermann, P. Maier-Komor, Nucl. Instrum. Methods B 99 (1995) 205.
[9] A. Blazevic, H.G. Bohlen, W.V. Oertzen, Phys. Rev. A 61 (2000) 032901.
[10] O. Vollmer, Nucl. Instrum. Methods 121 (1974) 373.
[11] K.B. Winterbon, Nucl. Instrum. Methods 144 (1977) 311.
[12] N. Bohr, Philos. Mag. 30 (1915) 581.
[13] H. Weick, H. Geissel, C. Scheidenberger, F. Attallah, T. Baumann, D. Cortina, M. Hausmann, B. Lommel, G. Münzenberg, N. Nankov, F. Nickel, T. Radon, H. Schatz, K. Schmidt, J. Stadlmann, K. Sümmerer, M. Winkler, H. Wollnik, Nucl. Instrum. Methods B 164-165 (2000) 168.
[14] P. Sigmund, Nucl. Instrum. Methods B 69 (1992) 113.

[15] A. Närmann, P. Sigmund, Phys. Rev. A 49 (1994) 4709.
[16] L. Glazov, P. Sigmund, Nucl. Instrum. Methods B 125 (1997) 110.
[17] Z.L. Miskovic, F.O. Goodman, W.K. Liu, Nucl. Instrum. Methods B 193 (2002) 26.
[18] P. Sigmund, A. Schinner, Nucl. Instrum. Methods B 195 (2002) 64.
[19] P. Sigmund, A. Schinner, Eur. Phys. J. D 12 (2000) 425.
[20] G. Schiwietz, P.L. Grande, Nucl. Instrum. Methods B 153 (1999) 1.
[21] T. Kaneko, Nucl. Instrum. Methods B 90 (1994) 58.
[22] N. Bohr, J. Lindhard, Mat. Fys. Medd. Dan. Vid. Selsk. 28 (No. 7) (1954) 1.
[23] O. Osmani, P. Sigmund, in: International Conference on Atomic Collisions in Solids, Krakow, Poland, 2010.
[24] J.P. Rozet, C. Stephan, D. Vernhet, Nucl. Instrum. Methods B 107 (1996) 67.
[25] P. Sigmund, A. Schinner, Eur. Phys. J. D 58 (2010) 105.